

A study of surface and interlayer structures of epitaxially grown group-III nitride compound films on Si(111) substrates by second-harmonic generation

This article has been downloaded from IOPscience. Please scroll down to see the full text article.

2003 J. Phys.: Condens. Matter 15 6537

(<http://iopscience.iop.org/0953-8984/15/38/020>)

View [the table of contents for this issue](#), or go to the [journal homepage](#) for more

Download details:

IP Address: 171.66.16.125

The article was downloaded on 19/05/2010 at 15:14

Please note that [terms and conditions apply](#).

A study of surface and interlayer structures of epitaxially grown group-III nitride compound films on Si(111) substrates by second-harmonic generation

Chau-Shiu Chen¹, Juh-Tzeng Lue^{2,4}, Chung-Lin Wu², Shangjr Gwo² and Kuang-Yao Lo³

¹ Department of Electrical Engineering, National Tsing Hua University, Taiwan, Republic of China

² Department of Physics, National Tsing Hua University, Taiwan, Republic of China

³ Department of Physics, National Chia-Yi University, Taiwan 30042, Republic of China

E-mail: jtlue@phys.nthu.edu.tw

Received 25 April 2003

Published 12 September 2003

Online at stacks.iop.org/JPhysCM/15/6537

Abstract

The symmetry behaviour of AlN/Si(111) and GaN/AlN/Si(111) structures grown by molecular beam epitaxy has been analysed by measuring the rotational dependence of the polarized second-harmonic generation (SHG) intensity for different polarized fundamental beams. The crystalline structure has also been checked by reflection high-energy electron diffraction, x-ray diffraction and photoluminescence spectroscopy. Considering various contributions of the nonlinear response from the bulk and interfaces, the interface strain implies an inhomogeneous intensity variation of SHG as a function of the surface azimuthal rotation angle ψ . This result provides a valuable illustration of the epitaxy quality and growth parameter characterization by a nondestructive method.

(Some figures in this article are in colour only in the electronic version)

1. Introduction

Gallium nitride and aluminium nitrides are the most promising wide-bandgap (3.4 and 6.2 eV, respectively) semiconductors for fabrication of short-wavelength opto-electronic devices. Due to the difficulty in obtaining large bulk GaN crystals, the nitride films are typically grown on several kinds of substrate such as sapphire, GaAs or silicon with different growth conditions. So far, the crystal growth techniques of the nitrides have been discussed in many experiments with some variables and different explainable viewpoints. Because of lattice mismatch between the deposit films and substrates, the buffer layer plays the important role of successful epitaxial growth. However, the quality and interface strain of the epitaxial films are often difficult to

⁴ Author to whom any correspondence should be addressed.

measure. In this work, AlN and GaN were deposited on Si(111) substrates by molecular beam epitaxy (MBE) and their structural quality was examined by several surface probe techniques. The detection of reflected SH generation has been illustrated to be a prominent method to measure the quality of nitride films deposited on Si(111) substrates.

Previously we have implemented SHG to calculate the dielectric constants of thin metallic films by generation of surface plasmons [1, 2] and to characterize the interface structures [3, 4]. SHG also provides valuable applications for investigating thin solid films [5, 6], such as formation of metal overlayers [7], surface disordering [8], surface melting [9], and amorphous to crystalline transformation [8]. The second-order nonlinear optical process precludes that SHG from the electric-dipole approximation is forbidden in media with inversion symmetry. The electric dipoles contribute to the SHG within a Thomas–Fermi screen length [2] just underneath the surface where the periodicity of the lattice is broken. Considering the noncentrosymmetric material, both the surface and bulk dipole contributions are involved in the SHG process.

Theoretical estimated values of the second-order susceptibility tensor element d_{33} of GaN are about 50 times larger than the d_{11} of quartz [10]. Several experimental studies have demonstrated that GaN crystalline film inherits a high nonlinear optical coefficient [11, 12]. The bulk effective second-order nonlinearity of AlN is also several times larger than that of quartz or KDP [13]. The noncentrosymmetric GaN and AlN hence can exhibit a sizable electric-dipole-allowed bulk second-order NLO response. As far as the centrosymmetric Si(111) crystal is concerned, it is known that there can be no electric-dipole contribution to the SHG away from the surface. The process of SHG from Si is governed by the high-order nonlinearity [14]. The bulk electric-quadrupole and magnetic-dipole nonlinearity of the surface and interface are the main contributions to the SHG of the wide-bandgap multilayer films [15]. Electric quadrupole nonlinearity can also be divided into bulk and surface parts. The latter is the result of the discontinuity of the normal component of the electric field at the surface. In this *ad hoc* prepared sample, the surface nonlinearity is dominated by the interfacial strain-induced dipole on account of the perfect bonds existing in the bulk volume of the film grown by MBE.

The reflection high-energy electron diffraction had been exploited for *in situ* monitoring of the stress relaxation for layer-by-layer MBE growth of III–V compounds [16–18], but the detection of the surviving strain in epitaxial films has still not been reported. In this work, we found that interface strain resulting in a large anharmonic potential can lead to an extra nonlinear optical response [19]. Many theories or experimental achievements specify the relation between the strain/stress and the azimuthal SH generation reflected from the epitaxial thin film on different substrates, such as Si, Ge and GaAs. Govorkov *et al* [20] delineated the theoretical dependence of inhomogeneous deformation of silicon surface layers and found the ratio of strain-induced and quadrupole contributions to second-harmonic intensity. Furthermore, Huang [21] employed Raman spectra and Fourier transformation and found the second-harmonic anisotropy dependent on the thickness of silicon oxide. Lyubchanskii *et al* [22] also reported that a p-polarized SH wave can be generated from a strain layer induced by either lattice misfit or dislocation while the s-polarized SH is generated only from a strain layer induced by dislocation. Many researchers focused on the strained interface problem due to surface oxide and heteroepitaxy. So far, studies of heteroepitaxial multilayer structure have not been observed. In this work, we implemented the optical SHG to diagnose the structure quality of III–V compound films deposited on silicon substrates by MBE.

2. Theory

In this system, noncentrosymmetric polar III–V compound films were grown on silicon wafers with inversion symmetry. The observed SH light is attributed to the response of surface layer by a sheet of electric dipole and the bulk incorporated with the magnetic dipole and electric

quadrupole. The reflected SH field observed from a multilayer system has to exploit Fresnel coefficients L_{ij} for multiple transmission and reflection of the fundamental and SH lights. For the fundamental field incident from medium 1 and generating SH in the nonlinear cubic medium 2 and then back to medium 1, the SH fields derived from Maxwell's equations with appropriate boundary conditions are given by [15, 23, 24]

$$\begin{aligned} E_S &= \frac{16\pi i\omega^2}{c^2(k_{1z} + k_{2z})} L_{yy}^{2\omega} P_y^{2\omega} \\ E_P &= \frac{16\pi i k_1 \omega^2}{c^2(k_2^2 k_{1z} + k_1^2 k_{2z})} (k_{2x} L_{zz}^{2\omega} P_z^{2\omega} + k_{2z} L_{xx}^{2\omega} P_x^{2\omega}) \end{aligned} \quad (1)$$

where $\mathbf{P}_i^{2\omega} = \mathbf{P}_{s,i}^{2\omega} + i \frac{\mathbf{P}_{b,i}^{2\omega}}{k_{s,z} + k_{2z}} F_i^{2\omega}$, and P_s and P_b refer to the surface and bulk harmonic polarizations, respectively. The subscript P (S) refers to the beam polarization parallel (perpendicular) to the plane of incidence. The \hat{z} -direction is along the normal of the surface, whereas the y -axis is taken to be perpendicular to the plane of incidence of the fundamental beam. In the above equations, the incident and nonlinear optical wavevectors are defined as $\mathbf{k}(\omega) = (k_x(\omega), 0, k_z(\omega))$ and $\mathbf{k}_s = 2\mathbf{k}(\omega) = (k_x(\omega), 0, k_{s,z}(\omega))$, respectively. The wavevectors \mathbf{k}_1 and \mathbf{k}_2 refer to the free waves propagating forward with the harmonic frequency 2ω , $L_{ii}^{2\omega}$ is the transmission Fresnel coefficient for the field, and $F_i(\omega) = \varepsilon_2(\omega)/\varepsilon'(\omega)$ for $i = z$ and $F_i(\omega) = 1$ for $i = x$ or y .

The SH polarizations can be contributed from the surface and the bulk. The electric dipole in the noninversion symmetry crystal is the dominant bulk term, while for centrosymmetric materials (e.g. the Si substrate) SH fields are embodied in an electric quadrupole and magnetic dipoles as given by

$$P_{b,i}^{2\omega} = \gamma \nabla_i (\mathbf{E} \cdot \mathbf{E}) + \zeta E_i \nabla_i E_i, \quad (2)$$

where γ and ζ are the nonzero bulk susceptibility tensor elements. The right-hand side of equation (2) includes the first term, a gradient vector which is independent of the orientation of principal axes, and the second term, an anisotropic contribution related to the azimuthal angle ψ .

On account of the interruption of crystal symmetry on the surface, there always exists a surface nonlinear source polarization (within the top 1–10 Å of the Thomson–Fermi screen length) of the form

$$P_s(2\omega) = \chi_s : E(\omega)E(\omega), \quad (3)$$

where χ_s is a theoretical surface susceptibility of a third-rank tensor. For all surfaces there are three independent terms, $\chi_{\perp\perp\perp}$, $\chi_{\perp\parallel\parallel}$, and $\chi_{\parallel\perp\parallel}$, in which \perp and \parallel refers to the direction perpendicular and parallel to the surface, respectively. For $3m$ symmetric surfaces there is an additional term $\chi_{\xi\xi\xi}$, where ξ is parallel to $[11\bar{2}]$ axis. According to the particular expression of nonlinear susceptibility of the crystal and contributions of the surface or bulk polarization, we can take advantage of coordinate transformation to find out the relation between the sample orientation and the intensity of SH fields.

In the SHG experiment of inversion symmetric Si(111) substrates, the nonlinear susceptibility is attributed from surface and bulk quadrupole terms. The surface term is dominantly arisen from the dipole sheet induced by interface strain. For either the p- or s-polarized pump radiation, the variation of the SH field on azimuthal angles for the Si(111) crystal surface with $3m$ symmetry are functions of the incident angle θ and the azimuthal angle φ as given by [25]

$$E_p^{2\omega} = a_p(\theta) + c_p \cos(3\varphi), \quad (4a)$$

$$E_s^{2\omega} = b_s \sin(3\varphi), \quad (4b)$$

where a_p , b_s , and c_p are linear combinations of the isotropic surface susceptibilities (via equation (3)) and their bulk values (via equation (2)) such as $\chi_{\perp\perp\perp} - \gamma$, $\chi_{\perp\parallel\parallel} - \gamma$, and $\chi_{\parallel\perp\parallel}$. The angle of rotation φ is measured between the plane of incidence and the $[2\bar{1}\bar{1}]$ direction in the (111) surface. For $a_p(\theta) = 0$, the generated SH is sixfold symmetry and for $a_p(\theta) = 1$ a threefold symmetry is expected. To the noncentrosymmetric films, the nonlinear polarization is prominently attributed from the bulk dipole moments. The noncentrosymmetric structure of AlN or GaN is different from the centrosymmetric Si(111) which belong to $6mm$ hexagonal close-packed and $3m$ diamond structures, respectively. The theoretical susceptibility χ is practically replaced by the experimental nonlinear coefficient d which is related to it by $2d_{ijk} = \chi_{ijk}$. The number of 3^3 matrix components d_{ijk} are reduced to 18 independent components d_{il} by considering the symmetry of $d_{ijk} = d_{ikj}$. We can contract the indices d_{ijk} to d_{il} by exploiting the formula $P_i = 2d_{il}F_l = 2d_{il}(1 - \frac{1}{2}\delta_{jk})(E_jE_k + E_kE_j)$. For the specific symmetry of AlN or GaN, the nonzero nonlinear optical coefficients are d_{15} , d_{31} , and d_{33} . In the ideal wurzite structure, these nonvanishing susceptibility tensor elements are related by $d_{15} = d_{31}$ and $d_{31} = -d_{33}/2$. For the p- or s-polarized fundamental beam, the bulk terms of the p- or s-polarized SH field at the incident angle θ can be written as

$$\begin{aligned} P_{p-p}^{(2)}(2\omega) &= 2(2d_{15} \cos\theta \sin\theta + d_{33} \sin^2\theta + d_{31} \cos^2\theta)E_0^2 \\ P_{s-p}^{(2)}(2\omega) &= 2d_{31}E_0^2 \\ P_{s-s}^{(2)}(2\omega) \quad \text{and} \quad P_{p-s}^{(2)}(2\omega) &= 0, \end{aligned} \quad (5)$$

where E_0 is the input electric field. No s-polarized SH wave can be generated from GaN and AlN films irrespective of whether the fundamental input is s- or p-waves.

AlN and GaN films grown on Si(111) substrate are inherited with nonvanishing tensor elements such as $d_{15} = d_{24}$, $d_{31} = d_{32}$ and d_{33} . The nonlinear optics (NLO) response in addition to a contribution from the bulk Si(111) also has a contribution from the electric dipoles of the deposited films and interfacial strain layer. The discrepancy in SH intensity between experimental and theoretical results in GaN or AlN bulk crystals suggests that the s-polarized SH field can be generated from the excitation of both p- and s-polarized pumping waves. Since the reflecting p-polarized SH field is independent of the azimuthal angle φ while it depends on the incident angle θ , we can derive the NLO response from the contributions of isotropic terms.

In epitaxially grown thin film structures, elastic strain occurs near the interface resulting from a misfit of the lattice constants of film and substrate, especially in a heteroepitaxial multilayer structure. The misfit factor can be expressed as $f = (a_f - a_s)/a_s$, where a_s and a_f are the lattice constants of the substrate and film, respectively. The mismatched lattice constants determine the thickness of the strained layer. The noncentrosymmetric dipole field induced by the strained layer implies an extra contribution to the nonlinear response. The theory describing nonlinear response due to inhomogeneous strain in crystals is based on the sp^3 -orbital model as expressed by Jha and Bloembergen [26]. They assumed only Coulomb interactions between atoms in the lattice are dominant, and merely adopted hydrogen-like atomic wavefunctions. Finally, the second-order nonlinear optical susceptibility of each unit cell was derived as in [20] for the strained layer as

$$\chi_{ijk}^{(2)} = -\frac{3\chi^{(1)}}{2E_g \sum_{\eta} \langle |\vec{d}|^2 \rangle_{\eta}} \sum_{\eta} \langle d_i^{\eta} d_j^{\eta} d_k^{\eta} \rangle_{\eta}. \quad (6)$$

Here d_i^{η} means a component of dipole moment; \vec{d} is one of the four covalent bonds (denoted by the symbol η) along the crystallographic axes. The equation in the summation takes the average over the η -bond ground state and can be exploited to yield the strain-induced NL susceptibility.

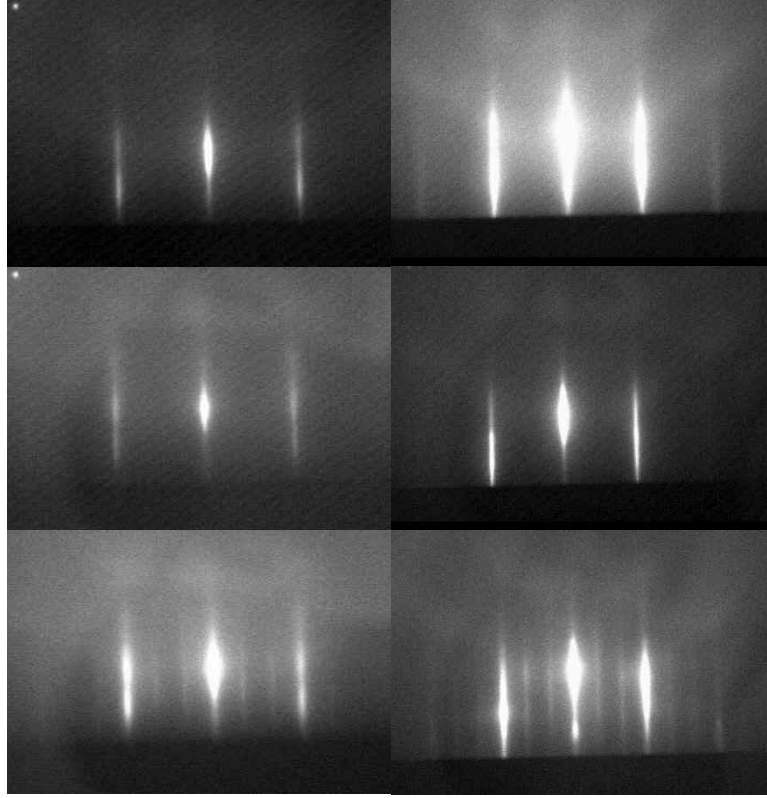


Figure 1. The three left-hand RHEED patterns show the AlN growth after 20 and 90 min of growth time and finally nitrogen-polarized (3×3) reconstruction after lowering the temperature to 520°C . The three right-hand RHEED patterns show the GaN grown on AlN/Si(111) after 10 and 100 min of growth time and finally nitrogen-polarized (3×3) reconstruction after lowering the temperature to 580°C .

Govorkov *et al* [20] expressed the azimuthal angle dependence of the p-polarized SHG for a p-wave incident beam by

$$I_{\text{p-p}} \sim [\chi_{xxx}^{(2)\text{IH}} \cos 3\varphi + \delta]^2, \quad (7)$$

where $\chi_{xxx}^{(2)\text{IH}}$ means the inhomogeneous strain-induced contribution to the NLO susceptibility, and δ is a linear combination of $\chi_{ijk}^{(2)\text{IH}}$ elements. Accordingly, the isotropic and anisotropic terms in equation (4) increase with the inhomogeneous strain. In [21], the nonvanishing elements of the second-order NLO susceptibility of the Si(111) strained lattice have been demonstrated.

3. Experiments

The films were grown on (111) Si substrates by MBE and simultaneously monitored by RHEED. After pre-cleaning and buffer-oxide etching (BOE), Si(111) substrates showed a good (7×7) reconstruction after thermal annealing in the ultra-high-vacuum chamber. The surface reconstruction ensures that the surface is clean and free from oxide and contamination of impurities. AlN and GaN films were subsequently grown on Si(111) substrates by heating

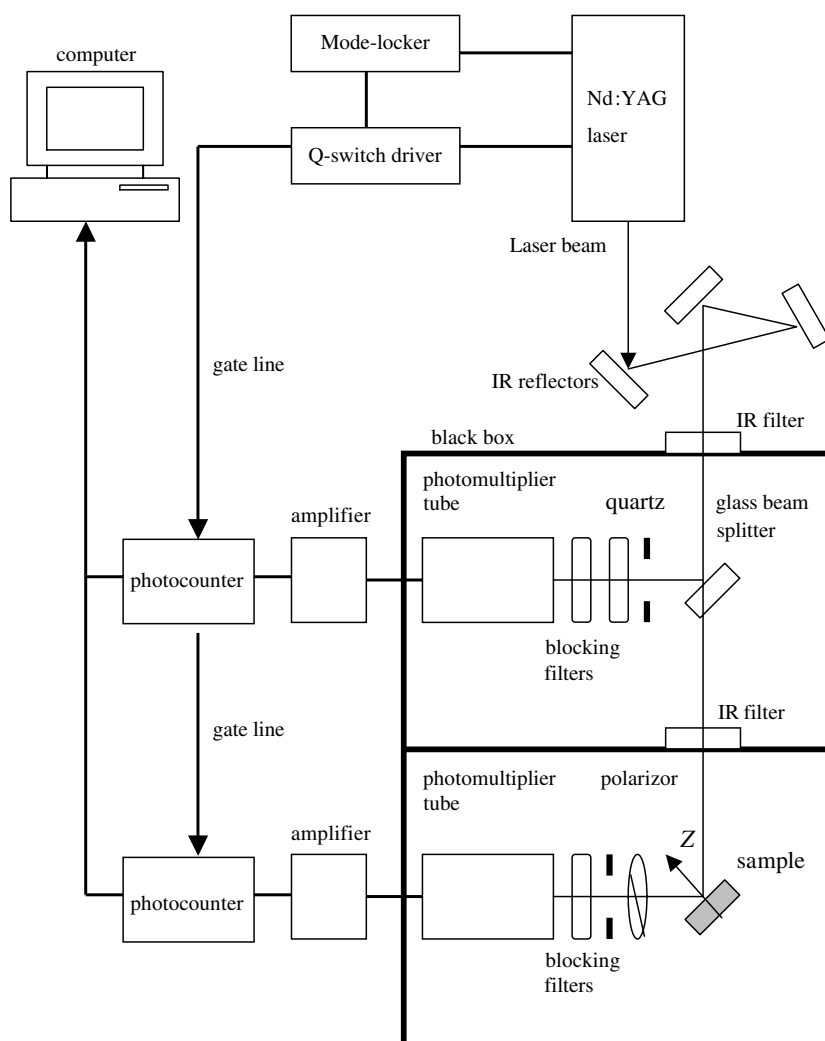


Figure 2. The set-up for the SHG experiment.

the aluminium and gallium sources to 1240 and 1140 °C respectively, with a nitrogen gas flow rate of 0.4 sccm. The substrate temperatures were kept at 940 and 700 °C to grow AlN and GaN films respectively. The growth time is 1.5–2 h with a thickness of about 200–300 nm as determined by the TEM and RHEED. The PL spectra ensure that the grown films are high quality and epitaxial. Figure 1 shows RHEED patterns of AlN and GaN, exhibiting a fine (3 × 3) reconstruction after lowering the substrate temperature to about 500–600 °C. This reconstruction pattern indicates that the grown GaN and AlN surfaces have the wurzite structure. The x-ray 2θ diffraction spectrum indicates the single-crystalline orientation of the film.

The experimental set-up for the SH generation measurement is sketched in figure 2. The source of the fundamental radiation is a passively mode-locked, Q -switched Nd:YAG laser (wavelength at 1064 nm) with a typical FWHM of 100 ps at a Q -switch repeating rate of 1 kHz. Due to the extremely narrow pulse width, the single-pulse energy can be reduced to as low as

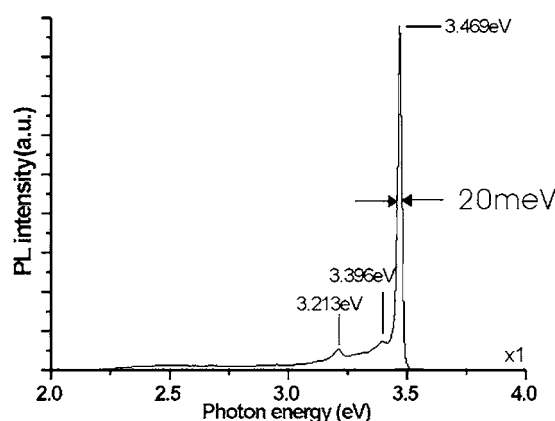


Figure 3. PL spectrum of GaN/AlN/Si(111) film measured at the sample temperature of 7 K.

0.5 mJ to immunize from any thermal destruction and black-body radiation of the film. The output of the laser passes through a glass beam splitter, which reflects 5% of the laser intensity on an AT-cut quartz plate, which is employed as a reference SHG standard. The straight beam light, on passing through a Schott glass filter, illuminates the sample surface, which is mounted on a computer-controlled step-motor. Firstly, the light reflected from the sample surface passes through a set of blocking filters, which only allow the SH wave to pass through. A computer-controlled stepping motor provides an automatic scanning of the ψ angles for the sample surface orientation. Finally, the SHG signal is detected by a photomultiplier tube and then recorded by a gated counter.

4. Results and discussion

Figure 3 shows the PL spectrum of the GaN/AlN/Si(111) film measured at a temperature of 7 K. We can see a peak of transition energy at 3.47 eV with a sharp linewidth (FWHM) of 20 meV, which fits the theoretical value of the GaN bandgap. Other peaks in the PL spectrum may arise from defects or dislocations according to the surface morphology of AFM images. Because of the poor matching in the lattice constant and different thermal expansion coefficients between AlN films and Si(111) substrates, it is well known that dislocations and strains ubiquitously spread in the III-V compounds during the growth processes. Both the dislocation densities are about 10^8 – 10^{10} cm^{-2} . It is necessary to monitor the growth conditions by *in situ* RHEED and by XRD after the growth for inspection of epitaxial quality.

To study the surface SHG, the fundamental s-polarized beam can be changed to p-wave by a set of three reflectors and the polarization of the reflected SH wave is detected. The beam alignment and the sixfold symmetries of the SHG pattern were examined by plotting the ϕ -scan patterns of the p-polarized input and p- and s-wave SHG outputs of Si(111) in the atmosphere as shown in figure 4. The theoretical fitting parameters are $a_p(\theta) = 0.019$, $c_p = 0.606$ for p-wave and $b_s = 0.257$ for s-wave, respectively, as expressed in equation (4). The nondistorted SH patterns certify the good alignment of the measurement.

Figure 5 shows the azimuthal second-harmonic intensity pattern taken from the AlN/Si(111) film. Owing to the high bandgap (6.2 eV) of the material, most of the infrared wave with wavelength $1.064 \mu\text{m}$ passes through the AlN film and reaches the interface of AlN and Si(111), and generates the SH field with the wavelength of $0.532 \mu\text{m}$, which radiates and

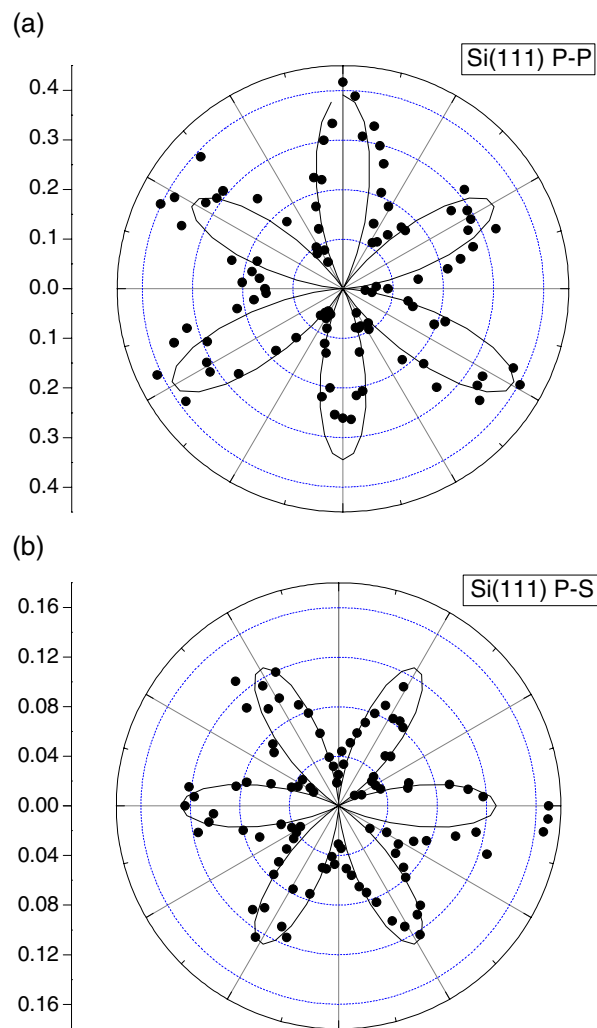


Figure 4. The p-input and s-output SHG patterns of Si(111) in the atmosphere. $a_p(\theta) = 0.019$ and $c_p = 0.606$ for p-polarized SHG, and b_s is 0.357 after the theoretical fitting.

transmits back to the air with negligible power loss. In this structure, the main contributions to the second-order nonlinear response come from three sources. One is from the dipole term of the bulk AlN film, the second is from the strain induced dipole term of the interfacial layer, and the third is from the electric quadrupole of the bulk Si(111) crystal. The bulk AlN contributes to the isotropic term a_p and the interface strain contributes to both a_p and c_p with the fitting value a_p and c_p being 0.021 and 0.715, respectively. Owing to the thin AlN buffer layer (200–300 nm), the contributions of SH polarization from the bulk and interface strain layer are limited. Apparently the s-polarized SH field signal (figure 5(b)) is much weaker than the p-polarized wave for a fundamental incident p-wave on the AlN bulk layer.

Figure 6 sketches the pattern of the reflected second-harmonic intensity depending on the azimuthal angle ψ from the GaN/AlN/Si(111) structure. The overlayer GaN film contributes to the second-order nonlinear response that comprises the total SHG intensity and

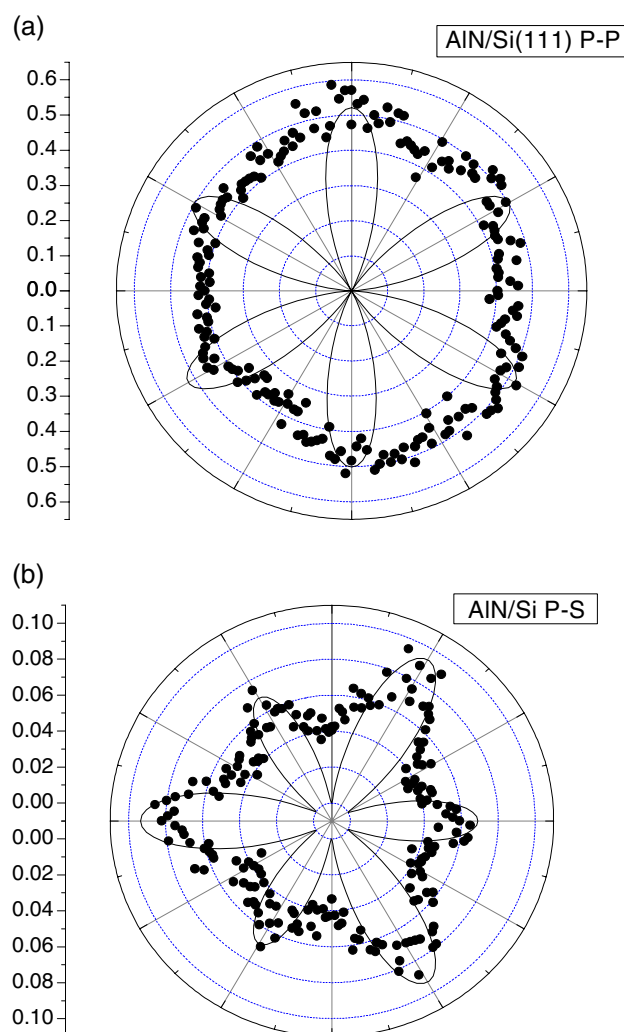


Figure 5. Azimuthal angle ψ -dependence on the pattern of reflected second-harmonic intensity from the AlN/Si(111) film. The solid curve represents the theoretical simulation.

the contribution from the interfacial dipole layer between the AlN and GaN films imposes an additional value. In this structure, the p-polarized SH intensity illustrates that the contribution from the isotropic term is greater than that of the anisotropic one. Consequently, the quality of GaN plays an essential role of yielding strong second-order nonlinear response [20] and results in the enhancement of a_p compared with the c_p in equation (4a).

The s-polarized SH response displayed in figure 6(b) has the same result as those of the p-polarized wave. Owing to the lack of the s-polarized contribution from both bulk III-V compounds, the p-in s-out SH field response is attributed to the nonlinear dipole susceptibilities of silicon and two interfaces of AlN/Si(111) and GaN/AlN. The growth of GaN on AlN increases the strain at the interface of AlN/Si(111) which contributes more effects of the isotropic a_p and isotropic c_p , resulting in a total increase of the SH intensity. Comparing the surface scans for the fundamental p-polarized incident beam, the s- and p-wave SHG patterns

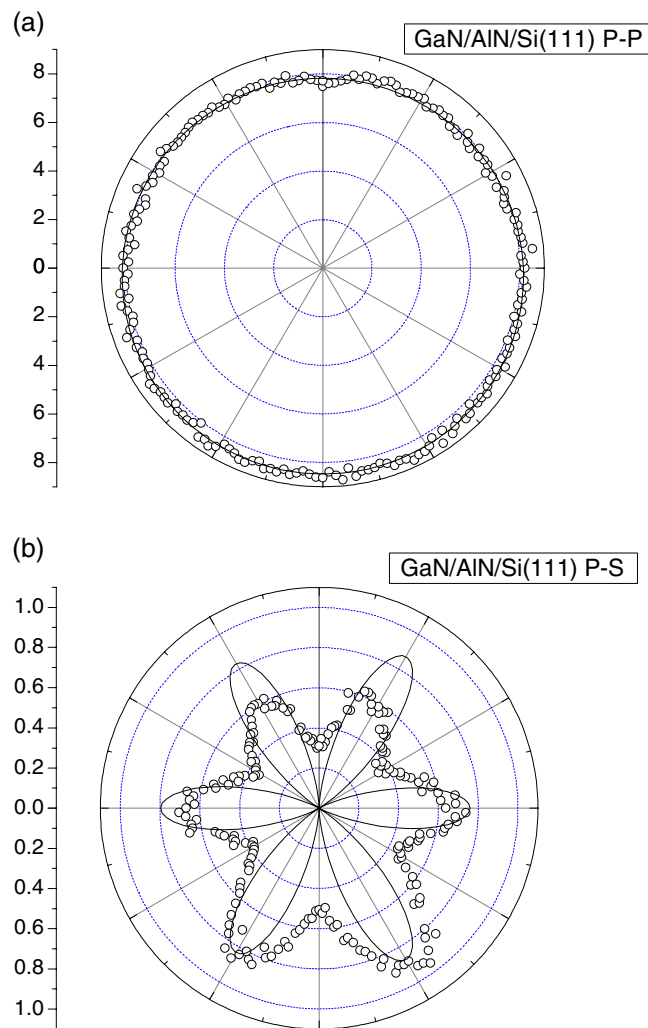


Figure 6. Azimuthal angle ψ -dependence of the pattern of the reflected second-harmonic intensity from the GaN/AlN/Si(111) film. The solid curve represents the theoretical simulation.

of GaN/AlN/Si(111) show the same enhancement at some orientations but are different for the *s*- or *p*-polarized SH pattern of AlN/Si(111). A plausible reason is that homogeneous deformations do not break the inversion symmetry of the cubic crystal. If the deformation of the interface is inhomogeneous, the characteristic value of nonlinear susceptibilities will be prominent in a certain orientation of the material. The susceptibility in the particular orientation is no longer the same as in the original structure and depends on the behaviour of the inhomogeneous deformation. If the value of the deformation depends on the depth of the interface along the surface normal, the inhomogeneous strain-induced second-order nonlinear susceptibility tensor will have the same nonvanishing components as the surface-dipole nonlinear susceptibility tensor because the symmetry of the strained layer is the same as that of the surface film.

Since the x-ray crystallography clearly reveals the epitaxial growth of the AlN film, we tacitly assume that the reason for the orientation-enhanced SH intensity pattern is the

effect of the nonuniform inhomogeneous interface strain induced by misfit of the lattice and dislocation as inspected from the AFM pictures. However, the interface of AlN/Si(111) does not have this effect because the Si(111) reconstruction generates the homogeneous base for the AlN film grown. Envisaging the experimental results of the SH enhancement at certain orientations, the p-polarized SH intensity might be dependent on a factor $g \cos^2(\Delta\phi)$, where g is a fitting constant, and $\Delta\phi$ is the deviation of incident angle from the strain direction ϕ_0 . The inhomogeneous strain introduces an enhanced anharmonic oscillation strength along a certain azimuthal direction.

5. Conclusions

In this scenario, we have successfully grown single-crystalline GaN films on silicon(111) substrates by a molecular beam epitaxial method via the introduction of an interfacial AlN layer for lattice matching. A pragmatic application in making blue light emitting diodes to be integrated with the well achieved very-large-scale-integrated silicon process is possible. The azimuthal angular scanning of optical second-harmonic generation (SHG) exploited as a nondestructive diagnosis to examine the interface quality can be readily applied in air.

A strain layer presented in the interface induces different anharmonic oscillation strength along a special crystal orientation resulting in anisotropic distribution for the surface scan of SH intensity. The surface term dominantly arises from the dipole sheet induced by interface strain. The deformation of the interface is inhomogeneous; the characteristic value of nonlinear susceptibilities will be prominent in a certain orientation of the material. Considering the large increase of the isotropic term of the surface scan of the SHG from GaN/AlN/Si samples as shown in figure 6, the p-s excitation is more effective than p-p excitation to examine the existence of inherited strain in epitaxial films. The sensitive surface SHG provides a clue to detect the surface strain inherited in the MBE crystal growth that cannot be elucidated by other surface analysis methods. Unfortunately, it is premature for us to provide any quantitative information on the so-called strain layer as extracted from the reported SHG experiments.

Acknowledgments

This work was supported from the National Science Council of the Republic of China under contract NSC92-2112-M-007- and from the Ministry of Education under contract 92-FA-04-AA.

References

- [1] Tzeng C C and Lue J T 1989 *Surf. Sci.* **216** 579–86
- [2] Tzeng C C and Lue J T 1989 *Phys. Rev. A* **39** 191
- [3] Lue J T, Lo K Y and Tzeng C C 1992 *IEEE J. Quantum Electron.* **38** 302
- [4] Lue J T and Dai C 1993 *Phys. Rev. B* **47** 13653
- [5] Shen Y R 1984 *The Principles of Nonlinear Optics* (New York: Wiley)
- [6] Tom H W K, Aumiller G D and Brito-Cruz C H 1988 *Phys. Rev. Lett.* **14** 1438
- [7] Shank C V, Yen R and Hirlimann C 1983 *Phys. Rev. Lett.* **51** 900–2
- [8] Heinz T F, Loy M M T and Thompson W A 1985 *J. Vac. Sci. Technol. B* **3** 1467–70
- [9] Akhmanov S A *et al* 1983 *Opt. Commun.* **47** 202–4
- [10] Levine B F 1973 *Phys. Rev. B* **7** 2600
- [11] Catalano I M, Cingolani A, Lugara M and Minafra A 1977 *Opt. Commun.* **23** 419
- [12] Ishidate T, Inoue K and Aoki M 1980 *Japan. J. Appl. Phys.* **19** 1641
- [13] Lin W P, Lundquist P M, Wong G K, Rippert E D and Ketterson J B 1993 *Appl. Phys. Lett.* **63** 2875
- [14] Akhmanov S A, Emel'yanov V I, Koroteev N I and Seminogov N I 1985 *Sov. Phys.—Usp.* **28** 1084–154

-
- [15] Tom H W K, Heinz T F and Shen Y R 1983 *Phys. Rev. Lett.* **51** 1983–6
 - [16] Grandjean N and Massies J 1997 *Appl. Phys. Lett.* **71** 1816
 - [17] Silverira J P and Briones F 1999 *J. Cryst. Growth* **201/202** 113
 - [18] Beresford R, Yin J, Tetz K and Chason E 2000 *J. Vac. Sci. Technol. B* **18** 1431
 - [19] Bottomley D J, Mito A, Fons P J, Niki S and Yamada A 1997 *IEEE J. Quantum Electron.* **33** 1294
 - [20] Govorkov S V, Emel'yanov V I, Koroteev N I, Petrov G I, Shumay I L and Yakolev V V 1989 *J. Opt. Soc. Am. B* **6** 1117
 - [21] Huang J Y 1994 *Japan. J. Appl. Phys.* **1** **33A** 3878
 - [22] Lyubchanskii I L, Dadoenkova N N, Lyubchanskii M I, Rasing Th, Jeong J W and Shin S C 2000 *Appl. Phys. Lett.* **76** 1848
 - [23] Bloembergen N, Chang R K, Jha S S and Lee C H 1968 *Phys. Rev.* **174** 813
Bloembergen N, Chang R K, Jha S S and Lee C H 1969 *Phys. Rev.* **178** 1528 (erratum)
 - [24] Feller M B, Chen W and Shen Y R 1991 *Phys. Rev. A* **43** 6778
 - [25] Sipe J E, Moss D J and van Driel H M 1987 *Phys. Rev. B* **35** 1129
 - [26] Jha S S and Bloembergen N 1968 *Phys. Rev.* **171** 891–8